Ultrafast Dynamic Control of Spin and Charge Density Oscillations in a GaAs Quantum Well

J. M. Bao,[1] L. N. Pfeiffer,[2] K.W. West,[2] and R. Merlin[1]
[1]*Focus Center and Department of Physics, The University of Michigan, Ann Arbor, Michigan 48109-1120, USA*
[2]*Bell Laboratories, Lucent Technologies, Murray Hill, New Jersey 07974, USA*
(Received 6 October 2003; published 8 June 2004)

We use subpicosecond laser pulses to generate and monitor in real time collective oscillations of electrons in a modulation-doped GaAs quantum well. The observed frequencies match those of intersubband spin- and charge-density excitations. Light couples to coherent density fluctuations through resonant stimulated Raman scattering. Because the spin- and charge-related modes obey different selection rules and resonant behavior, the amplitudes of the corresponding oscillations can be independently controlled by using shaped pulses of the proper polarization.

DOI: 10.1103/PhysRevLett.92.236601 PACS numbers: 72.25.Fe, 42.65.Dr, 73.21.Fg, 78.47.+p

Spin currents are the most common source of magnetism and, since spin cannot be described in classical terms, it is apparent that the majority of magnetic phenomena are ultimately a manifestation of quantum behavior. While this fact has been known for a very long time, it is only recently that methods to generate spin-polarized currents have attracted much attention, driven mainly by the possibility that novel quantum effects and devices may be uncovered [1]. Next to electrical methods, the generation of magnetic currents by optical injection has now become a very active area of research. Here III-V semiconductor quantum wells (QWs), particularly those belonging to the AlGaAs/GaAs system, play an important role owing to the spin-polarized nature of their valence band [2]. We note that these heterostructures have been used for many years to produce, by means of photoexcitation, incoherent spin-polarized electron sources for applications in nuclear and high energy physics [3]. More recently, injection of a pure spin current has been achieved in a GaAs QW through interference of one- and two-photon absorption processes [4].

In this work we use ultrafast light pulses to induce coherent density oscillations associated, separately, with the spin and charge degrees of freedom of a quasi-two-dimensional electron gas (2DEG) contained in a single GaAs QW. Studies of the ultrafast dynamics of low-lying levels of a QW have been previously reported [5–14]. Our results distinguish themselves from those studies in that we are able to differentiate collective (many-particle) from single-particle behavior and observe many-electron dynamics in real time (for recent theoretical work on intersubband excitations, see [15,16]). The method we use to generate and control the spin and charge oscillations is stimulated Raman scattering (RS) by intersubband excitations. Given that *spontaneous* RS is one of the main tools for probing 2DEG properties and, in particular, the quantum Hall effects [17,18], our results hold promise for elucidating the coherent dynamics of these and other 2DEG phenomena.

Our sample, grown by molecular beam epitaxy on a (001) GaAs substrate, is a 400 Å one-sided modulation-doped GaAs single QW sandwiched between $Al_{0.3}Ga_{0.7}As$ barriers; see Fig. 1(a). The 2DEG originates from electrons initially bound to those Si donors in the barriers which are closest to and migrate to the QW. To reduce ionized impurity scattering and thereby enhance the mobility, these donor atoms are separated from the 2DEG by a 10^3-Å-thick undoped spacer [20]. A schematic energy level diagram is shown in Fig. 1(b). The excitations pertinent to our work are intersubband transitions associated with the lowest-lying states of the QW. We used transport measurements at 4.2 K to determine the sample mobility $\mu = 2.9 \times 10^6$ cm^2/V s and the 2DEG areal density $\sigma_0 \approx 1.9 \times 10^{11}$ cm^{-2} for which the corresponding Fermi energy is $E_F \approx 7$ meV. The latter value is consistent with the width of the main photoluminescence (PL) feature in Fig. 1(c) [21]. From the PL data, we also get ~1.512 eV for the renormalized QW band gap [22]. Figure 1(d) shows schematically the long-wavelength limit of the excitation spectrum involving the two lowest-lying subbands. The wave vector $\mathbf{q}$ is perpendicular to the growth axis [001]. The spectrum consists of the single-particle (SP_{01}) continuum delimited by $E_{01} \pm \hbar q k_F/m$ and, at small wave vectors, the collective spin-density (SD_{01}) and charge-density (CD_{01}) resonances [23]. Here, k_F is the Fermi wave vector, m is the electron effective mass, and $E_{01} = (E_1 - E_0)$. As shown in Fig. 1(e), Raman data of our QW at $\mathbf{q} = 0$ (vertical transitions) reveal the expected three distinct features at 2.60 (SD_{01}), 2.85 (SP_{01}) and 3.31 (CD_{01}) THz. These results are typical of high-mobility samples [24–26]. Here, z denotes the axis normal to the layers and x' (y') is along the [110] ([1$\bar{1}$0]) direction [19]. We notice that the charge (spin) related peak appears in polarized (depolarized) spectra, i.e., when the incident and scattered polarizations are parallel (orthogonal) to each other. This reflects the fact that the charge (spin) density mode transforms like the symmetric A_1 (antisymmetric A_2) representation of the D_{2d} point group of the QW [24].

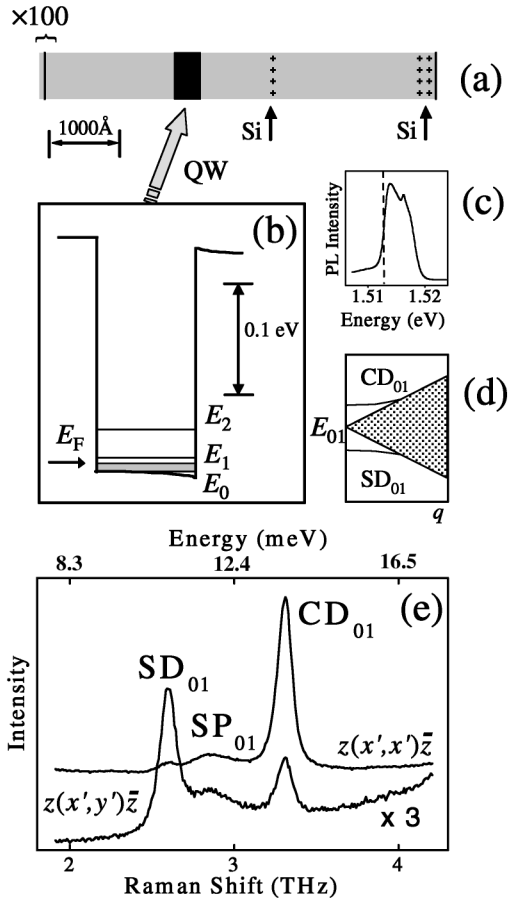

FIG. 1. (a) Sample structure showing Si donors (+) introduced by δ doping. The black and gray areas denote, respectively, GaAs and $Al_{0.3}Ga_{0.7}As$. A smoothing superlattice consisting of 100 periods of 30 Å GaAs and 100 Å $Al_{0.3}Ga_{0.7}As$ was grown on top of the substrate, which is on the left-hand side of the diagram. The two doping layers close to the sample surface help pull the conduction band edge to very near the 2DEG Fermi level at the position of the Si donors close to the QW. (b) Energy level diagram. (c) Photoluminescence spectrum obtained at 7 K with 0.01 W/cm^2 of the 4880 Å Ar line. The dashed line denotes the QW gap. The weaker peak at ~1.516 eV is not associated with the 2DEG. (d) Wave vector dependence of intersubband excitations for $q \ll k_F$. The shaded area denotes single-particle excitations SP_{01}. (e) Raman spectra recorded in the backscattering configuration [19]. The (continuous wave) laser energy is 1.556 eV.

Time domain pump-probe experiments were performed at ~7 K in the reflection geometry using a mode-locked Ti:sapphire laser which provided ~50–65 fs pulses at a repetition rate of 82 MHz. The stronger pump pulse generates coherent oscillations in the electron density, which modify the 2DEG optical constants and, thereby, perturb the weaker probe pulse which follows behind. The laser beams, of average power 5–20 mW (pump) and 2.5 mW (probe), penetrated the crystal along the z axis (hence, $\mathbf{q} = 0$) and were focused onto a 300-μm-diameter spot. The pump beam was either circularly or linearly polarized, along x', while the incident probe beam was linearly polarized, along y'. We measured the pump-induced change in the field of the reflected probe beam, $\delta\mathbf{E}_R$, as a function of the time delay between the two pulses. To obtain $\delta\mathbf{E}_R$, also known as the coherent scattered field, we determined separately the pump-induced shift of the polarization angle of the reflected probe field, $\delta\theta$, and the differential reflectivity $\delta R \propto |\mathbf{E}_R + \delta\mathbf{E}_R|^2 - |\mathbf{E}_R|^2 \approx 2\mathbf{E}_R \cdot \delta\mathbf{E}_R$ ($\mathbf{E}_R$ is the reflected probe field when the pump is turned off). $\delta\theta$ was gained from differential magnetic Kerr measurements using the scheme described in [27], which gives an output signal proportional to $\mathbf{E}_R \times \delta\mathbf{E}_R$. As discussed below, symmetry dictates that $\delta\mathbf{E}_R$ must be perpendicular (parallel) to $\mathbf{E}_R$ and, hence, that $\delta R \equiv 0$ ($\delta\theta \equiv 0$) for spin (charge) density excitations. To enhance effects due to the 2DEG, we tuned the central energy of the pulses to a range where the spontaneous Raman cross section exhibits a pronounced enhancement; see the inset of Fig. 2(a). The positions of the maxima, at ~1.542 and ~1.552 eV, are consistent with those of the incoming and outgoing resonances [24] with heavy-hole excitons associated with the third lowest QW state of energy E_2.

The time-delay dependence of the reflected probe signal, reproduced in Fig. 2, shows well-resolved oscillations. The top and bottom traces of Fig. 2(a) represent, respectively, the normalized differential reflectivity and $\delta\theta$. After removal of the slowly decaying electronic background, we used linear prediction methods [28] to determine the number of oscillators and their parameters. This procedure gives three modes and fits such as those of Fig. 2 which reproduce quite accurately the experimental traces. The frequencies of the two lowest modes agree extremely well with those of SD_{01} and CD_{01} from the Raman spectra in Fig. 1(e) and, on this basis, we assign them to coherent spin- and charge-density oscillations. The weaker single-particle peak was only vaguely distinguished in the time-domain data. Our experiments show that the SD_{01} mode can be excited only if the pump beam is circularly polarized [Fig. 2(a), bottom trace], whereas the CD_{01} amplitude is largest for linearly polarized pump pulses. This selectivity, as well as the fact that the amplitude of the oscillations depends strongly on the central energy of the pulses (see below), opens the road for coherent control studies. SD_{01} and CD_{01} behave also quite differently *vis-à-vis* the probe detection scheme. While the CD_{01} contribution dominates the modulated intensity [Fig. 2(a), top trace], SD_{01} leads mainly to a rotation of the probe polarization. Hence, $\delta\mathbf{E}_R$ is mostly perpendicular (parallel) to the incident beam for spin (charge) oscillations. The appearance of the dominant charge-density modes in the bottom trace of Fig. 2(a) and the depolarized Raman spectrum of Fig. 1(e) is attributed to a polarization leakage (notice that, relative to CD_{01}, the time-domain signal for SD_{01} is significantly smaller than the Raman signal). The remaining feature at 3.97 THz, labeled CD_{12}, is ascribed to charge-density transitions of *photoexcited* electrons involving the states of energies E_1 and E_2 [29]. We believe that the presence of these carriers,

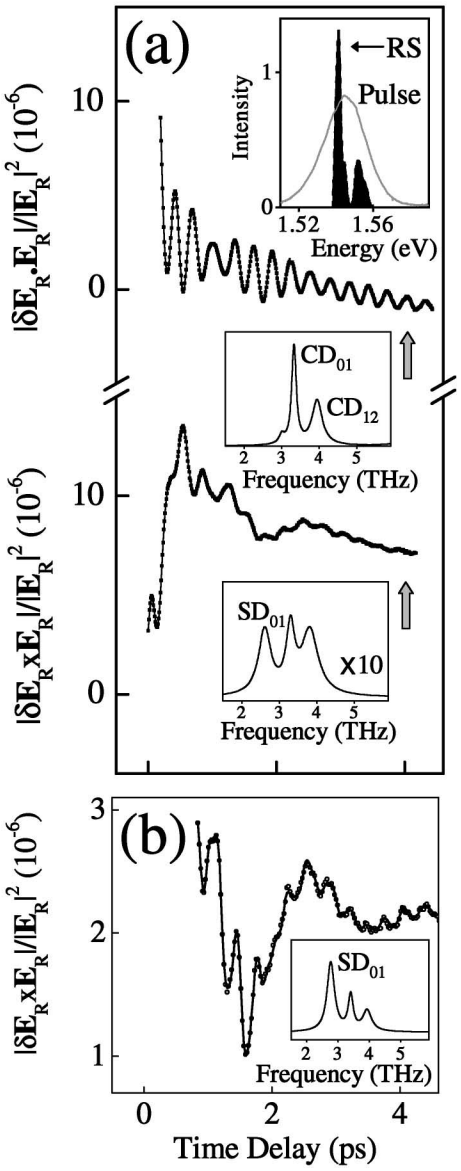

FIG. 2. (a) Time-resolved differential reflectivity (top) and magnetic Kerr (bottom) data. Curves are linear prediction fits [28]. The associated insets are Fourier transform intensity spectra showing peaks due to charge- and spin-density oscillations. The top and bottom traces were obtained, respectively, with linearly and circularly polarized pump pulses. For the top (bottom) trace, the scattered field, $\delta \mathbf{E}_R$, is parallel (perpendicular) to the polarization of the incident probe beam. Inset: Dependence of the spontaneous CD_{01} Raman cross section on laser energy. Results obtained with a continuous wave Ti:sapphire laser at ~ 1 W/cm^2. Also shown is the energy spectrum of the light pulses centered at 1.545 eV. (b) Same as the bottom trace of (a) but for pulses centered at 1.536 eV.

providing additional decay channels, is the reason why the width of the peaks is somewhat larger in the time-domain data. Our assignment of CD_{12} is supported by the calculated QW level spacing and the fact that it exhibits the same selection rules as CD_{01}. Moreover, additional results (not reported here) show that the strength of CD_{12} increases with increasing pump power in a manner that is consistent with estimates of the photoinduced population of the E_1 subband. We note that, for a given average power density, the E_1 population is expected to be significantly larger for impulsive excitation. This explains why the RS results reveal no evidence of CD_{12} scattering. Finally, we emphasize the fact that the amplitude of both spin- and charge-density oscillations depends strongly on the photon energy. The data of Fig. 2(b), obtained at a central energy that is near the maximum of the spin-density RS resonance, exhibit relatively much stronger spin-density oscillations.

The correlation we find between time-domain and spontaneous RS results, particularly in regard to the positions of the peaks, the resonant behavior, and the selection rules (see below), strongly indicates that stimulated RS is the mechanism responsible for the coherent 2DEG oscillations. Following work on impulsive stimulated RS by phonons [30,31], the coherent interaction between the electromagnetic field and 2DEG density fluctuations is described, with minor modifications, by the same effective Hamiltonian which accounts for spontaneous intersubband RS [32]. Phenomenologically, we write the coupling energy as

$$H_S = \frac{1}{8\pi} \sum_{jl} \int F_j^*(\omega_1) \gamma_{jl}(\omega_1, \omega_2) F_l(\omega_2) d\omega_1 d\omega_2 + \text{c.c.}, \tag{1}$$

where $\mathbf{F}(\omega)$ is the Fourier transform of the (pump or probe) electric field $\mathbf{F}(t)$ and

$$\gamma_{jl} = C_{jl}(\hat{\sigma}_{\mathbf{q}\uparrow} + \hat{\sigma}_{\mathbf{q}\downarrow}) + iS_{jl}(\hat{\sigma}_{\mathbf{q}\uparrow} - \hat{\sigma}_{\mathbf{q}\downarrow}). \tag{2}$$

Here $\hat{\sigma}_{\mathbf{q}s} = \sum_{\mathbf{k},mn} c^+_{\mathbf{k}s,n} c_{(\mathbf{k}+\mathbf{q})s,m}$ are density fluctuation operators, $c^+_{\mathbf{k}s,n}$ ($c_{\mathbf{k}s,n}$) is the electron creation (annihilation) operator for the state $|\mathbf{k}s, n\rangle$ of wave vector $\mathbf{k}$, spin component s, and subband index n, and C_{jl} (S_{jl}) is the Raman tensor describing the coupling to charge (spin) density fluctuations (for notation clarity, we ignore the dependence of the coupling constants on the subband index). Note that H_S commutes with the total spin of the 2DEG, and that the signs of the spin-up and spin-down operators are the same for C_{jl} but different for S_{jl}. We also recall that, due to the combination of spin-orbit coupling and quantum confinement, the spin of the holes mediating the scattering process and, thus, the electron spin quantization axis are perpendicular to the layers [33]. Since the symmetries of charge and spin excitations are A_1 and A_2, the relevant tensor components for light polarized in the plane of the layers are of the form $C_{x'x'} = C_{y'y'}$ and $S_{x'y'} = -S_{y'x'}$ (all other components vanish). Accordingly, and in agreement with our experimental findings, spin oscillations can be excited only by circularly polarized light whereas both linearly and circularly polarized light couple to the charge-density mode.

The following single-particle analysis provides a simple physical picture of, both, the screening behavior

of the two types of collective modes and the associated coherent states created by the laser pulses. Following an impulsive excitation with $\mathbf{q} = 0$, the wave function of an electron initially in the state $|\mathbf{k}s, 0\rangle$ of the lowest subband becomes, to lowest order in the pump electric field, $\Psi \approx |\mathbf{k}s, 0\rangle \exp(-iE_0 t/\hbar) + \sum_{n\neq 0} \alpha_{ns} |\mathbf{k}s, n\rangle \exp(-iE_n t/\hbar)$, where α_{ns} are constants proportional to the intensity of the pulses ($|\alpha_{ns}| \ll 1$). Hence, the quasi-2DEG density for a given spin polarization varies as

$$\delta\sigma_s(\mathbf{r}, t) \equiv \langle \hat{\sigma}_{\mathbf{q}=0,s} \rangle \approx \sum_{\substack{n\neq 0 \\ k<k_F}} \alpha_{ns} \langle \mathbf{r}|\mathbf{k}s, n\rangle \langle \mathbf{k}s, 0|\mathbf{r}\rangle e^{-i(E_n - E_0)t/\hbar} + \text{c.c.} \quad (3)$$

From (2), we have that $\alpha_{n\uparrow} = \pm \alpha_{n\downarrow}$, where the plus (minus) sign is for charge (spin) excitations. Thus, the effect of an optical pulse is to create *coherent* density oscillations for which the spin-up and spin-down components are either in phase (charge-density mode) or 180° out of phase (spin-density mode). Given that the two contributions add up for charge excitations (i.e., $\delta\sigma_\uparrow = \delta\sigma_\downarrow$), these plasmonlike modes experience a restoring field whereas spin excitations remain unscreened since the corresponding motion does not change the net density ($\delta\sigma_\uparrow + \delta\sigma_\downarrow = 0$). From (1) and the expression for the dielectric tensor $\varepsilon_{jl} = \langle \partial^2 H/\partial E_j E_l \rangle$, it follows that the coherent oscillations lead to a time-varying modulation of the optical constants and, because of the symmetry properties of C_{jl} and S_{jl}, that $\delta\mathbf{E}_R$ and the reflected probe beam must be along the same direction for charge, but perpendicular to each other for spin excitations. These selection rules are consistent with the experimental observations.

Acknowledgement is made to the donors of The Petroleum Research Fund, administered by the ACS, for partial support of this research. Work also supported by the NSF Focus Physics Frontier Center.

[1] S. A. Wolf, D. D. Awschalom, R. A. Buhrman, J. M. Daughton, S. von Molnár, M. L. Roukes, A. Y. Chtchelkanova, and D. M. Treger, Science **294**, 1488 (2001).
[2] See, e.g., P. Y. Yu and M. Cardona, *Fundamentals of Semiconductors* (Springer, Berlin, 1996), Chap. 2.
[3] T. Omori *et al.*, Phys. Rev. Lett. **67**, 3294 (1991), and references therein.
[4] M. J. Stevens, A. L. Smirl, R. D. R. Bhat, A. Najmaie, J. E. Sipe, and H. M. van Driel, Phys. Rev. Lett. **90**, 136603 (2003).
[5] T. Elsaesser and M. Woerner, Phys. Rep. **321**, 253 (1999).
[6] J. N. Heyman, R. Kersting, and K. Unterrainer, Appl. Phys. Lett. **72**, 644 (1998).
[7] T. Asano, M. Tamura, S. Yoshizawa, and S. Noda, Appl. Phys. Lett. **77**, 19 (2000).
[8] R. A. Kaindl *et al.*, Phys. Rev. Lett. **86**, 1122 (2001).
[9] P. C. M. Planken, M. C. Nuss, I. Brener, K. W. Goossen, M. S. C. Luo, S. L. Chuang, and L. Pfeiffer, Phys. Rev. Lett. **69**, 3800 (1992).
[10] C. Waschke, H. G. Roskos, R. Schwedler, K. Leo, H. Kurz, and K. Köhler, Phys. Rev. Lett. **70**, 3319 (1993).
[11] A. Bonvalet, J. Nagle, V. Berger, A. Migus, J. L. Martin, and M. Joffre, Phys. Rev. Lett. **76**, 4392 (1996).
[12] D. Some and A. V. Nurmikko, Phys. Rev. B **53**, R13 295 (1996).
[13] N. A. Fromer, C. Schüller, C. W. Lai, D. S. Chemla, I. E. Perakis, D. Driscoll, and A. C. Gossard, Phys. Rev. B **66**, 205314 (2002).
[14] N. A. Fromer, C. E. Lai, D. S. Chemla, I. E. Perakis, D. Driscoll, and A. C. Gossard, Phys. Rev. Lett. **89**, 067401 (2002).
[15] C. A. Ullrich and M. E. Flatté, Phys. Rev. B **66**, 205305 (2002).
[16] J. Li and C. Z. Ning, Phys. Rev. Lett. **91**, 097401 (2003).
[17] H. D. M. Davies, J. C. Harris, J. F. Ryan, and A. J. Turberfield, Phys. Rev. Lett. **78**, 4095 (1997).
[18] S. Luin, V. Pellegrini, A. Pinczuk, B. S. Dennis, L. N. Pfeiffer, and K. W. West, Phys. Rev. Lett. **90**, 236802 (2003), and references therein.
[19] We use the standard Porto notation: $a(b, c)d$ indicates that the incident (scattered) light propagates along the a (d) axis, and that its polarization vector is along b (c).
[20] L. N. Pfeiffer, K. W. West, J. P. Eisenstein, K. W. Baldwin, and P. Gammel, Appl. Phys. Lett. **61**, 1211 (1992).
[21] M. S. Skolnick *et al.*, Phys. Rev. Lett. **58**, 2130 (1987).
[22] A. Pinczuk, J. Shah, R. C. Miller, A. C. Gossard, and W. Wiegmann, Solid State Commun. **50**, 735 (1984).
[23] J. C. Ryan, Phys. Rev. B **43**, 12 406 (1991).
[24] For a review of Raman studies in quantum wells, see A. Pinczuk and G. Abstreiter, in *Light Scattering in Solids V*, Topics in Applied Physics Vol. 66, edited by M. Cardona and Güntherodt (Springer, Berlin, 1989), Chap. 4; A. Pinczuk, Adv. Solid State Phys. **32**, 45 (1992).
[25] A. Pinczuk, S. Schmitt-Rink, G. Danan, J. P. Valladares, L. N. Pfeiffer, and K. W. West, Phys. Rev. Lett. **63**, 1633 (1989).
[26] D. Gammon, B. V. Shanabrook, J. C. Ryan, D. S. Katzer, and M. J. Yang, Phys. Rev. Lett. **68**, 1884 (1992).
[27] S. A. Crooker, D. D. Awschalom, and N. Samarth, IEEE J. Sel. Top. Quantum Electron. **1**, 1082 (1995).
[28] H. Barkhuijsen, R. De Beer, W. M. M. J. Bovée, and D. van Ormondt, J. Magn. Reson. **61**, 465 (1985); F. W. Wise, M. J. Rosker, G. L. Millhuser, and C. L. Tang, IEEE J. Quantum Electron. **23**, 1116 (1987).
[29] For RS results on intersubband transitions of photoexcited electrons, see A. Pinczuk, J. Shah, A. C. Gossard, and W. Wiegmann, Phys. Rev. Lett. **46**, 1341 (1981); T. A. Perry, R. Merlin, B. V. Shanabrook, and J. Comas, Phys. Rev. Lett. **54**, 2623 (1985).
[30] R. Merlin, Solid State Commun. **102**, 207 (1997).
[31] T. E. Stevens, J. Kuhl, and R. Merlin, Phys. Rev. B **65**, 144304 (2002).
[32] M. V. Klein, in *Light Scattering in Solid*, Topics in Applied Physics Vol. 8, edited by M. Cardona (Springer, Berlin, 1975), Chap. 4.
[33] See, e.g., R. W. Martin, R. J. Nicholas, G. J. Rees, S. K. Haywood, N. J. Mason, and P. J. Walker, Phys. Rev. B **42**, 9237 (1990).